CrossMark

ORIGINAL ARTICLE

Body wave attenuation characteristics in the crust of Alborz region and North Central Iran

M. Farrokhi · H. Hamzehloo

Abstract Attenuation of P and S waves has been investigated in Alborz and north central part of Iran using the data recorded by two permanent and one temporary networks during October 20, 2009, to December 22, 2010. The dataset consists of 14,000 waveforms from 380 local earthquakes ($2 < M_L < 5.6$). The extended coda normalization method (CNM) was used to estimate quality factor of P (Q_P) and S waves (Q_S) at seven frequency bands (0.375, 0.75, 1.5, 3, 6, 12, 24 Hz). The Q_P and Q_S values have been estimated at lapse times from 40 to 100 s. It has been observed that the estimated values of Q_P and Q_S are time independent; therefore, the mean values of Q_P and Q_S at different lapse times have been considered. The frequency dependence of quality factor was determined by using a power-law relationship. The frequency-dependent relationship for Q_P was estimated in the form of $(62 \pm 7)f^{(1.03 \pm 0.07)}$ and $(48 \pm 5)f^{(0.95 \pm 0.07)}$ in Alborz region and North Central Iran, respectively. These relations for Q_S for Alborz region and North Central Iran have estimated as $(83 \pm 8)f^{(0.99 \pm 0.07)}$ and $(68 \pm 5)f^{(0.96 \pm 0.05)}$, respectively. The observed low Q values could be the results of thermoelastic effects and/ or existing fracture. The estimated frequency-dependent relationships are comparable with tectonically active regions.

M. Farrokhi
Department of Physics, Faculty of Science,
Hormozgan University, Bandar Abbas, Iran

H. Hamzehloo (✉)
Seismology Research Center, International Institute of Earthquake
Engineering and Seismology (IIEES), Tehran, Iran
e-mail: hhamzehloo@iiees.ac.ir

1 Introduction

Studying the seismic hazard and evaluating and predicting the strong ground motions require the knowledge of seismic wave attenuation. It is well known that some of the major uncertainties in earthquake hazard analysis are caused by uncertainties in seismic wave attenuation. Attenuation of seismic waves is an important parameter for determination of source parameters, physical properties of the media, seismic hazard assessment, and simulation of seismic waveform (Pulli 1984; Mukhopadhyay and Tyagi 2007). Moreover, the knowledge of attenuation properties within the media is required for investigation of earth structure and seismotectonic activity (Singh and Herrmann 1983; Jin and Aki 1988; Del Pezzo et al. 1995; Bianco et al. 2002). Tectonic activities can change the stress fields, which will result in the geomorphological deformation within the media and cause microfractures and brittle zone and fault zones. These fractures can change the attenuation properties of media. Therefore, a good physical agreement can be expected between attenuation properties, seismicity, and tectonics.

Seismic wave's amplitudes decrease as travel distance increases, due to some phenomena like

geometrical spreading, scattering attenuation, intrinsic attenuation, etc. The attenuation of seismic waves except the geometrical spreading effect can be quantified by the inverse of a dimensionless quantity called quality factor Q (Q^{-1}). Attenuation (Q^{-1}) is defined in terms of the fractional loss of energy per cycle of oscillation (Knopoff 1964; Lay and Wallace 1995). The attenuation of seismic waves (Q^{-1}) is the combination of the effects of scattering attenuation (Q_{Sc}^{-1}) and intrinsic absorption (Q_i^{-1}): $Q^{-1} = Q_{Sc}^{-1} + Q_i^{-1}$. Intrinsic absorption is due to the conversion of kinematic seismic energy into heat due to anelastic properties of media (Jackson and Anderson 1974). The scattering attenuation is an elastic process in which energy of seismic waves does not dissipated but is redistributed due to the existing inhomogeneities within the media. Scattering of seismic waves is responsible for the generation of the later parts of seismograms that follows direct P and S waves, which are named coda waves (Aki 1969; Sato and Fehler 2008; Sato et al. 2012).

Aki (1969) proposed coda waves that are scattered waves by inhomogeneities within the lithosphere. A single backscattering model of S waves was introduced to formulate the decay rate of coda wave's envelope with the assumption of collocation of source and receiver (Aki and Chouet 1975). Later, the single isotropic scattering model was introduced for non-collocated source and receiver situations (Sato 1977). Coda normalization method (CNM) was proposed based on the similarity between source and site effects of S and coda waves, for individual estimation of shear wave quality factor (Aki 1980). Using CNM, the source and site effects can be eliminated by division of S wave amplitude by the S coda amplitude, and attenuation (Q^{-1}) can be individually estimated. Radiative transfer theory (RTT) was introduced into seismology to formulate higher-order scattering (Wu 1985). Zeng (1991) introduced a hybrid approximation for RTT, which describes the energy pattern versus time and distance. Based on RTT, Aki (1992) concluded that coda waves are mainly composed of backscattering S waves or conversion of P to S wave. Later, the extended CNM was proposed for P wave's quality factor estimation based on the similarity of source effect of P and S waves for low to moderate earthquakes (Yoshimoto et al.

1993). A more reliable approximation of RTT was introduced by Paasschens (1997), which shows better agreement with the exact solution of RTT compared to Zeng (1991). This approximation has been used to estimate attenuation and source parameters for different regions (Sens-Schönfelder and Wegler 2006; Ugalde et al. 2010).

In this study, the attenuation properties of P and S waves are investigated in Alborz region and North Central Iran. These regions are among the most populated areas of Iran with a population of more than 20 million. The capital of Iran, Tehran, as well as many important industrial areas are located within the studied area (Fig. 1). The study area has experienced some destructive earthquakes in the past (Ambraseys and Melville 1982). This region is categorized as high to very high seismic hazard zone (BHRC 2007). A temporary network (TN) has been installed for a period of 14 months after occurrence of a moderate magnitude earthquake (M_L 4.0) in the vicinity of Tehran on October 17, 2009. Data provided by TN have been combined with the data of two existing permanent networks to increase the ray coverage. Finally, the collected data were used to investigate the attenuation properties of direct waves within the studied areas.

The attenuation of this region was estimated by several investigators using different methods (Motazedian 2006; Kamalian et al. 2007; Rahimi et al. 2010; Motaghi and Ghods 2012; Naghavi et al. 2012; Farrokhi et al. 2015). In this study, we estimated attenuation of direct P and S waves using extended CNM (Aki 1980; Yoshimoto et al. 1993). Our new dataset provides a more reliable estimation of Q_P and Q_S by considering 69 stations and 380 earthquakes. The lapse time dependency of estimated Q values has been investigated using 61 time windows from 40 to 100 s.

Fig. 1 **a** Studied area, active faults in the Alborz region and North ▶ Central Iran. Locations of Seismic stations and earthquakes have been plotted with *triangles* and *circles*. The *inverse triangles* are IRSC stations, *white triangles* are the broadband seismic stations of IIEES, and *yellow triangles* are the stations of TN. *Thick black V-shape line* shows the approximate boundary of Alborz and Central Iran regions. *Red star* shows the location of October 17, 2009, Tehran-Ray earthquake. The Damavand volcano has been shown. **b** Ray path of the used waveforms is plotted at each region
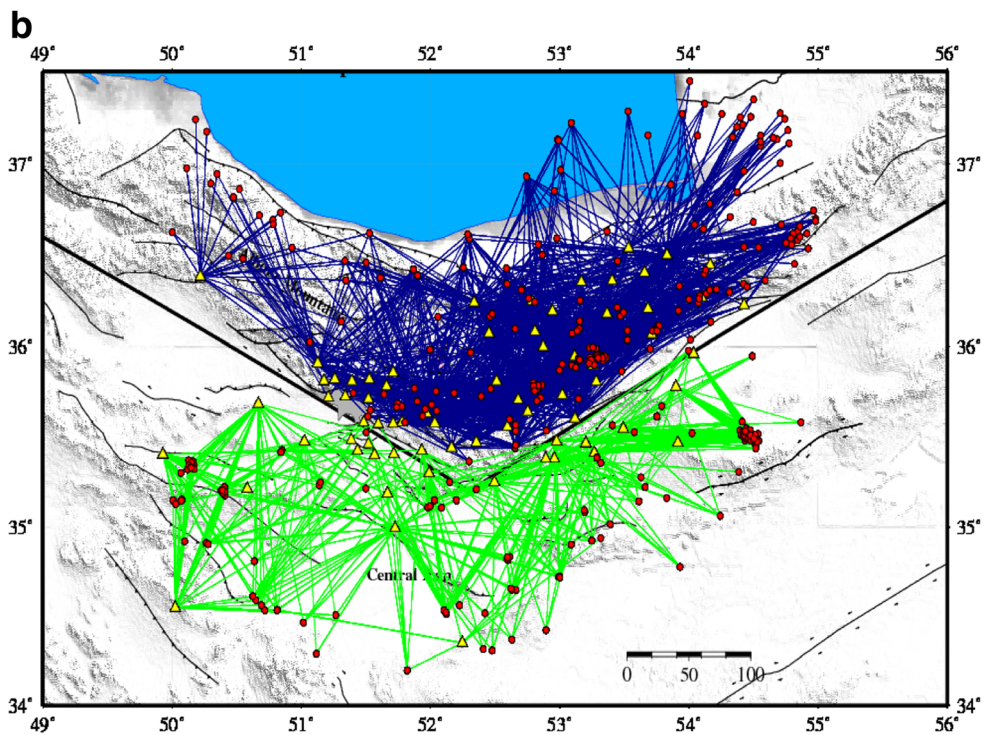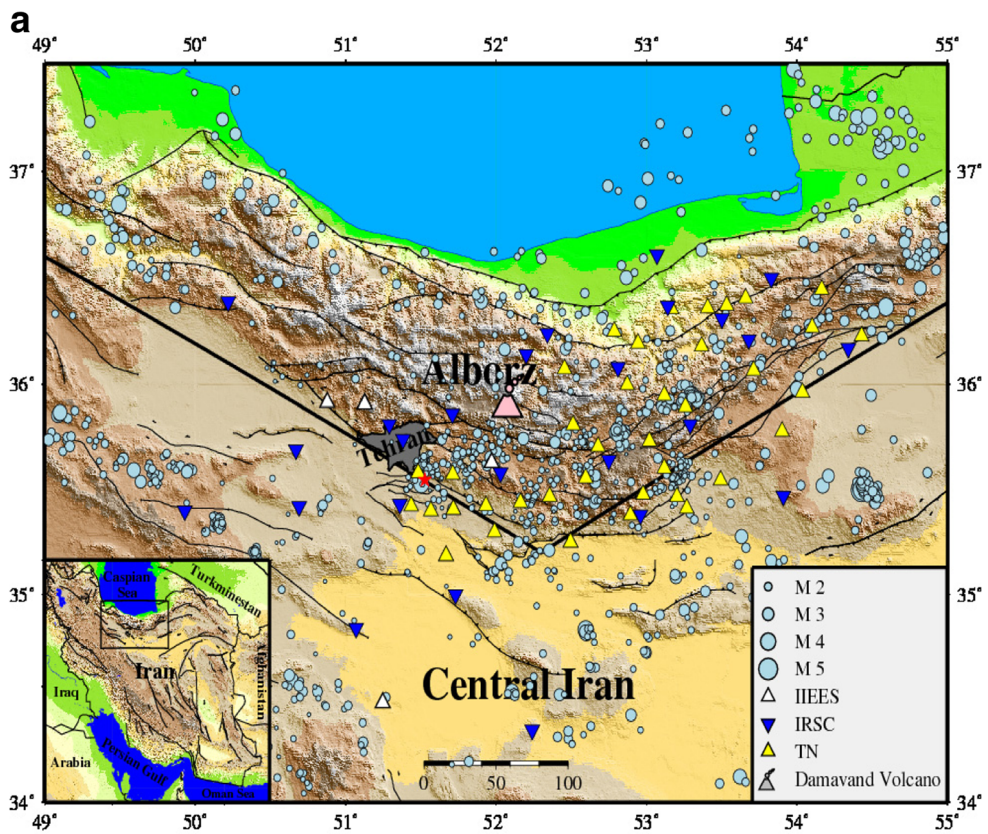
2 Tectonic setting and seismic activity

Alborz region, which is seismically active with E-W trending mountain belt, is a folded and faulted area extended for a distance of 960 km across the northern part of Iran (Farrokhi et al. 2015). This region is bounded to the Caspian Sea Block from the north and the Central Iranian block from the south. Its active tectonic was developed due to three tectonic stages. The first stage was the collision process between the Central Iranian block and Eurasia starting in the late Triassic that caused the closure of Paleo-Tethys Ocean (Stöcklin 1974; Jackson and McKenzie 1984). This stage followed by an extension stage caused andesitic eruption and volcanic rocks in central Alborz. The third tectonic stage was compression phases due to the Arabia-Eurasia continental collision, which results in the closure of Neo-Tethys oceanic lithosphere started in late Eocene (Guest et al. 2007). This collision-related compression affects the Northern Iran and Caspian basin and caused acceleration of tectonic processes and shortening in early to late Miocene (Ballato et al. 2011). Ballato et al. (2011) has suggested a two-stage collision process for Arabia-Eurasia collision, soft collision process for initial continental collision (36 Ma), and hard collision process (20–17.5 Ma) due to the arrival of unstretched Arabian continental lithosphere in the collision zone.

The V-shaped structure of the Alborz Mountains results in a redistribution of the tectonic forces along this range. The strikes of the Alborz range vary from N110° E in the western part to N80° E in the eastern part. The existing faults of the region are mostly parallel to the range (Allen et al. 2003). North-south shortening of 5 mm/year has been reported across Alborz region between Central Iran and South Caspian basin (Vernant et al. 2004). The total amount of shortening of 30 km has been reported for this range since early Pliocene (Allen et al. 2003). Ritz et al. (2006) mentioned the clockwise rotation for South Caspian block. The arcuate shape of the central part of Alborz region toward Central Iran makes its microseismicity and existed stresses complicated to understand. The existence of Damavand volcano in the center of Alborz region exceeds the complexity of stresses affecting the region (Fig. 1a). Damavand volcano is known as a dormant volcano which is the highest summit of Iran (5670 m). The first volcanic activity of Damavand started at 1.8 Ma, and the youngest eruptive products are lava flows which dated to ca. 7 ka (Davidson et al. 2004).

The study area has experienced several large destructive earthquakes with magnitude greater than 7 from 4th BC to 1830 (Ambraseys and Melville 1982). The most important instrumentally recorded earthquakes, which occurred within or near this region, are the 1962 Buin Zahra earthquake with magnitude M_W 7.2, the 2002 Changureh (Avaj) earthquake with magnitude M_W 6.5, the 2004 Firozabad Kojor earthquake with magnitude M_W 6.3, and the 2007 Kahak-Qom earthquake with magnitude M_W = 5.9 (Farrokhi et al. 2015). The nearest event, which occurred near Tehran and recorded by modern seismic instruments, was the October 17, 2009, Tehran-Ray earthquake with magnitude M_L 4.0 (Fig. 1).

3 Data

We have used data recorded by one temporary and two permanent networks. The TN operated for a period of about 14 months from October 20, 2009, to December 22, 2010. The data recorded by permanent networks of International Institute of Earthquake Engineering and Seismology (IIEES) and Iranian Seismological Center (IRSC) have been used in order to increase the ray coverage. We have used five broadband velocity seismometers of IIEES and 26 short-period velocity seismometers of IRSC. The TNs consisting of 38 velocity seismometers were installed by IIEES. Seismometers of IIEES, TN, and IRSC, which are used in this study, are Güralp CMG-3T, CMG-6TD, and Kinemetrics (SS1) with sampling rates of 50 and 100 and 50 Hz, respectively. The frequency responses of IIEES, TN, and IRSC networks were flat from 50 Hz to 0.01, 0.1, and 1 Hz, respectively. All stations were connected to an external GPS for time synchronization.

The extracted events have been merged, preprocessed, and located using HYPOCENTER subroutine (Lienert and Havskov 1995). The study area has been divided into North Central Iran and Alborz region (Fig. 1). To estimate the quality factor of P and S waves, we have considered 380 well-located earthquakes. The criteria for selection of these events are based on the (i) recorded at least at eight stations and (ii) epicentral error of less than

8 km. The selected events have local magnitudes (M_L) from 2 to 5.6 and hypocentral distances from 30 to 130 km (Fig. 2). It is worth noting that events with a magnitude less than 4 have been used to estimate the P wave attenuation.

4 Methodology

The source spectral amplitudes of P (S_P), S (S_S), and coda waves (S_c) have the following relation:

$$S_P(f) \propto S_S(f) \propto S_c(f, t_c) \tag{1}$$

where f and t_c are the frequency and lapse time (determined from the origin time of event), respectively. Aki (1980) proposed CNM in which S wave's amplitude becomes normalized by coda waves. This method assumes a proportionality between the site effect and the coda for S waves (Tsujiura 1978; Sato et al. 2012) and proportionality of source spectra of S and coda waves. Source, site, and instrument effects can be eliminated by this method. Therefore, anelastic attenuation can be individually estimated (Aki 1980). Yoshimoto et al. (1993) have extended the CNM for estimation of P wave attenuation based on the similarity between source spectra of P to S waves for earthquakes with low to moderate

Fig. 2 M_L magnitude versus hypocentral distance distribution

magnitude range. Equations 2 and 3 have been used to estimate Q_P and Q_S values (Yoshimoto et al. 1993):

$$\left\langle \ln\left[\frac{A_P(f,r)}{A_C(f,t_c)} GS(r)\right]\right\rangle_{r\pm\Delta r} = -\frac{\pi f}{V_P Q_P(f)} r + \text{const}_P(f) \tag{2}$$

$$\left\langle \ln\left[\frac{A_S(f,r)}{A_C(f,t_c)} GS(r)\right]\right\rangle_{r\pm\Delta r} = -\frac{\pi f}{V_S Q_S(f)} r + \text{const}_S(f) \tag{3}$$

where A_P and A_S are the maximum amplitudes of direct P and S waves at hypocentral distance of r, respectively (Fig. 3b). A_c is the average amplitude of coda wave at lapse time t_c (measured from the origin time of the seismic event). The geometrical spreading correction factor, $GS(r)$, is considered to be (r) for $r < 90$ km and $(90\,r)^{0.5}$ for $r > 90$ km. The V_p and V_s are the average velocities of P and S waves, which are calculated from travel time curve of Pg and Sg seismic phases as 6 and 3.5 km/s, respectively. The symbol $\langle\rangle_{r\pm\Delta r}$ is the spatial averaging within the hypocentral distance of $r \pm \Delta r$ ($\Delta r = 10$ km). Const$_p$ and const$_s$ are constants and can be determined by regression analysis of Eqs. (2) and (3).

Aki (1980) assumed that the amplitude of the direct body waves will become independent of azimuth when averaged over many events with a wide range of directions from the station. The average value has no systematic geographical variation (Aki 1980). With this assumption, we could smooth out the radiation pattern differences when the measurements are made over a large enough number of earthquakes with good azimuthal coverage. On the other hand, it has also been reported that if the window length of P and S waves became much greater than earthquake source time function, the effect of radiation pattern will be eliminated (Del Pezzo et al. 2006). The source time functions are less than 1.5 s for most of events. We have used a time window with a width of 5 s to determine the maximum amplitude of P and S waves, which is much greater than source time function of most of events (1.5 s). Therefore, the effect of radiation pattern on the maximum amplitude of direct waves is negligible.

We have considered lapse times greater than twice the arrival times of S waves ($2t_s$) to have uniform energy distribution for scattered coda waves (Aki and Chouet 1975; Rautian and Khalturin 1978).
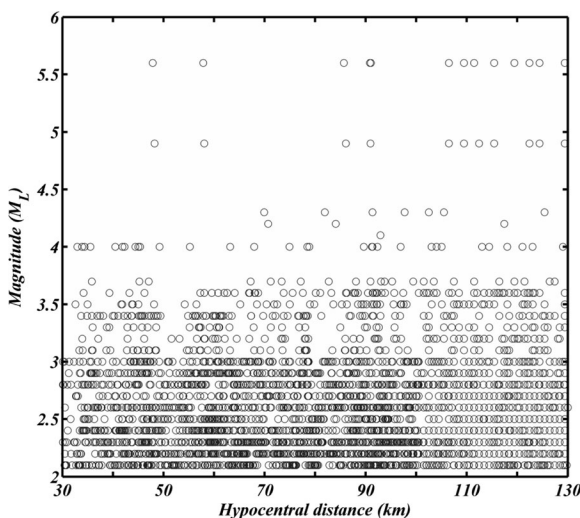
5 Data processing

The extended CNM has been used to estimate the attenuation of direct P and S waves. We have used vertical component data for the determination of P wave's amplitude. The horizontal components have been used for S wave and coda wave amplitude determination. A cosine taper with a width of 5% of the data length has been applied to both ends of each waveform after removing the trend and baseline correction (Fig. 3a). Then, the waveform has been bandpass filtered using different frequency bands (Table 1). The window length of 5 s has been considered for determination of P and S wave amplitudes, which starts from the arrival time of P and S waves, respectively (Fig. 3b). The P and S wave window lengths were considered to be much longer than the source time function of most of the events. The maximum amplitudes of filtered seismogram have been considered as A_P and A_S at the selected time window of P and S waves, respectively.

A 5-s window length has been considered before the arrival time of P waves for determination of noise amplitude. The root-mean-square (RMS) value of the noise time window was used as an estimate of the noise amplitude (Fig. 3b). We have considered a window of 5 s for estimation of coda wave amplitude (A_c), which centered at lapse time t_c ($t_c > 2t_s$). Then, the RMS of selected window has been calculated and considered as coda wave amplitude (A_c). We have considered 61 coda time windows moving from 40 to 100 s to investigate the lapse time dependence of Q_P and Q_S (Fig. 3b). The first window starts from 37.5 to 42.5 s, and the last window starts from 97.5 to 102.5 s. In this study, the signal-to-noise ratios of 3, 4, and 2 have been considered for P, S, and coda waves, respectively.

The ratios of A_P/A_c and A_S/A_c were calculated for all lapse times for each seismogram. It was observed that the normalized amplitudes of A_P/A_c and A_S/A_c increase as lapse time increases (Fig. 3d). The values of Q_P and Q_S have been estimated (at each lapse time) from slope of linear regression of Eqs. (2 and 3), versus hypocentral
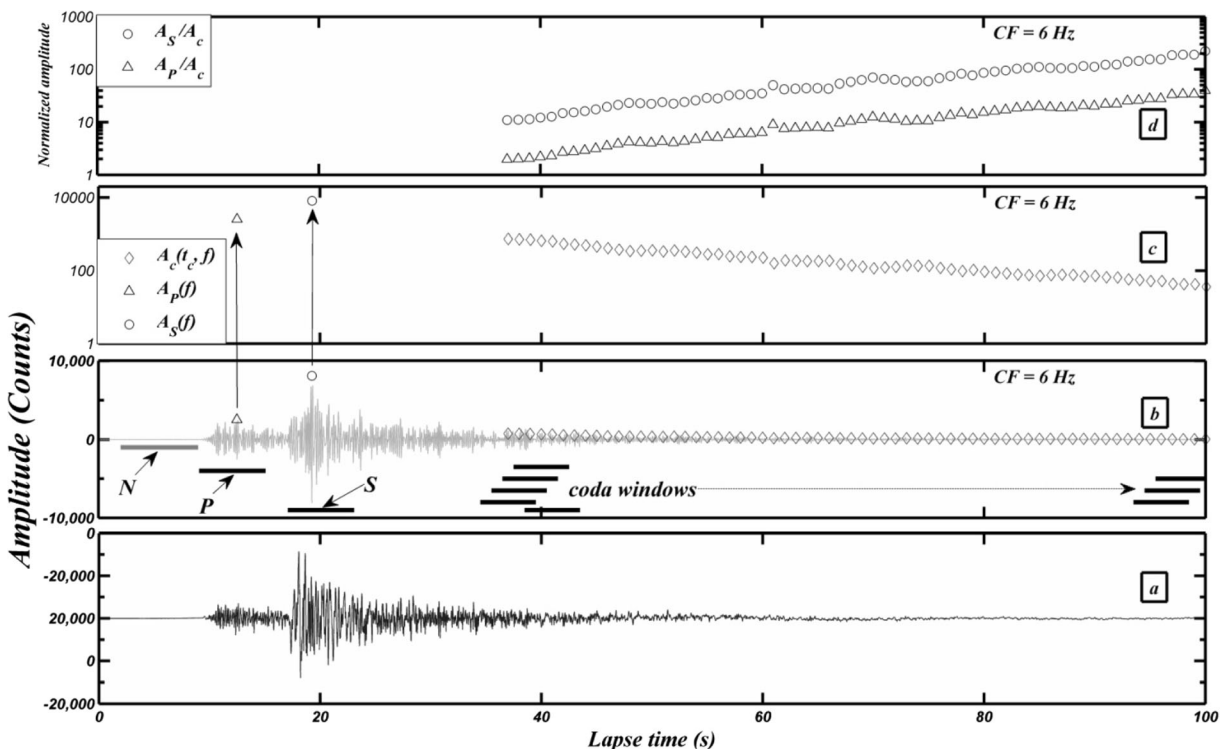

Fig. 3 a Raw seismogram located at Damavand station (IIEES) with hypocentral distance of 56 km with a magnitude of 4.0. **b** Butterworth bandpass-filtered seismogram at 6 Hz. Noise, P, S, and 61 coda windows for determination of noise, A_P, A_S, and A_c are shown with N, P, S, and coda windows, respectively. **c** A_P, A_S, and A_c are plotted by *triangle*, *circle*, and *diamonds*, respectively. **d** The normalized amplitudes of A_P/A_c and A_S/A_c are shown with *triangles* and *circles* at the used lapse times, respectively

Table 1 Frequency bands used in this study

Frequency band (Hz)	Central frequency (Hz)	Alborz Region		North Central Iran	
		Q_P	Q_S	Q_P	Q_S
0.25–0.50	0.375	18 ± 11	24 ± 7	15 ± 5	31 ± 2
0.50–1.0	0.75	40 ± 20	75 ± 8	32 ± 25	49 ± 12
1.0–2.0	1.5	149 ± 36	147 ± 13	94 ± 31	85 ± 34
2.0–4.0	3.0	195 ± 83	271 ± 17	193 ± 70	173 ± 64
4.0–8.0	6.0	394 ± 155	460 ± 40	256 ± 137	442 ± 95
8.0–16.0	12.0	861 ± 193	858 ± 67	425 ± 122	756 ± 115
16.0–24.0	24.0	1342 ± 570		911 ± 157	

distance, respectively (Fig. 4). The R-square criteria (R^2) have been considered to be greater than 0.7 and 0.5 for Q_S and Q_P estimations, respectively.

It is well known that coda waves sample the attenuation properties inside a spheroidal region around the station (Aki and Chouet 1975; Pulli 1984). The similarity between the decay rates of coda waves at different stations, which result in the similar increase rate for normalized amplitude of A_P/A_c and A_S/A_c, is related to the attenuation properties around these stations. Therefore, data from different stations with similar coda trend can be simultaneously analyzed (Kim et al. 2004). Several studies have reported the combination of data, which have provided by spatially distributed stations with distances up to 300 km (Frankel et al. 1990; Chung and Lee 2003; Mahood et al. 2009). We have observed the same trend for the normalized amplitudes of A_P/A_c and A_S/A_c at different stations inside eastern and western parts of Alborz region and North Central Iran (Fig. 5). Therefore, the combined information of all stations in each region has been considered for Q estimation. The average of the normalized amplitude of P and S waves has been plotted at the right-end image of Fig. 5 for Alborz (top) and Central Iran (bottom) regions.

6 Results and discussion

Attenuation of P and S waves has been studied by using 380 local earthquakes, which occurred within the Alborz region and North Central Iran. A total number of 14,000 waveforms have been used to estimate attenuation properties of P and S waves by using the extended CNM (Yoshimoto et al. 1993).

The decay rate of the normalized amplitude contains the effects of geometrical spreading as well as attenuation. It is accepted that the body wave's geometrical spreading (GS) is related to travel distance. However, this effect becomes a little complicated, when the analysis considers the maximum amplitude of body wave. The effect of GS has been considered based on a two-step approach: (i) $GS(r) = r$ for $r \leq h_m$ and (ii) $GS(r) = (r.h_m)^{0.5}$, and h_m may be considered to be twice the thickness of crust (Hermanns and Kijko 1983; Kumar et al. 2005; Mahood et al. 2009; Hamzehloo et al. 2010). The Moho depth has been reported to be between 45 and 52 km for this region (Sodoudi et al. 2009; Radjaee et al. 2010; Rahimi et al. 2014). Therefore, h_m was considered as 90 km. Motaghi and Ghods (2012) have reported that the GS effect changes at distance of greater than 80 km.

The attenuation of P (Q_P^{-1}) and S waves (Q_S^{-1}) was estimated at each lapse time by using Eqs. 2 and 3. The estimated Q_S^{-1} and Q_P^{-1} values are nearly lapse time independent for lapse times between 40 and 100 s (Fig. 6). Therefore, the mean values of estimated Q_S^{-1} and Q_P^{-1} have been considered at each frequency band at lapse times from 40 to 100 s (Table 1). A frequency-dependent relationship in the form of $Q(f) = Q_0 f^n$ has been considered. These relationships are tabulated in Table 2 for both Alborz region and North Central Iran. Figure 7 shows variation of Q_P^{-1} and Q_S^{-1} versus frequency for both regions.

We have also used synthetic seismogram to verify this lapse time independency. For this purpose, we have used Paasschens (1997) approximation of RTT to synthesize the envelopes of seismograms at different hypocentral distances (10, 20, 30, 40,…, 110 km; Fig. 8).
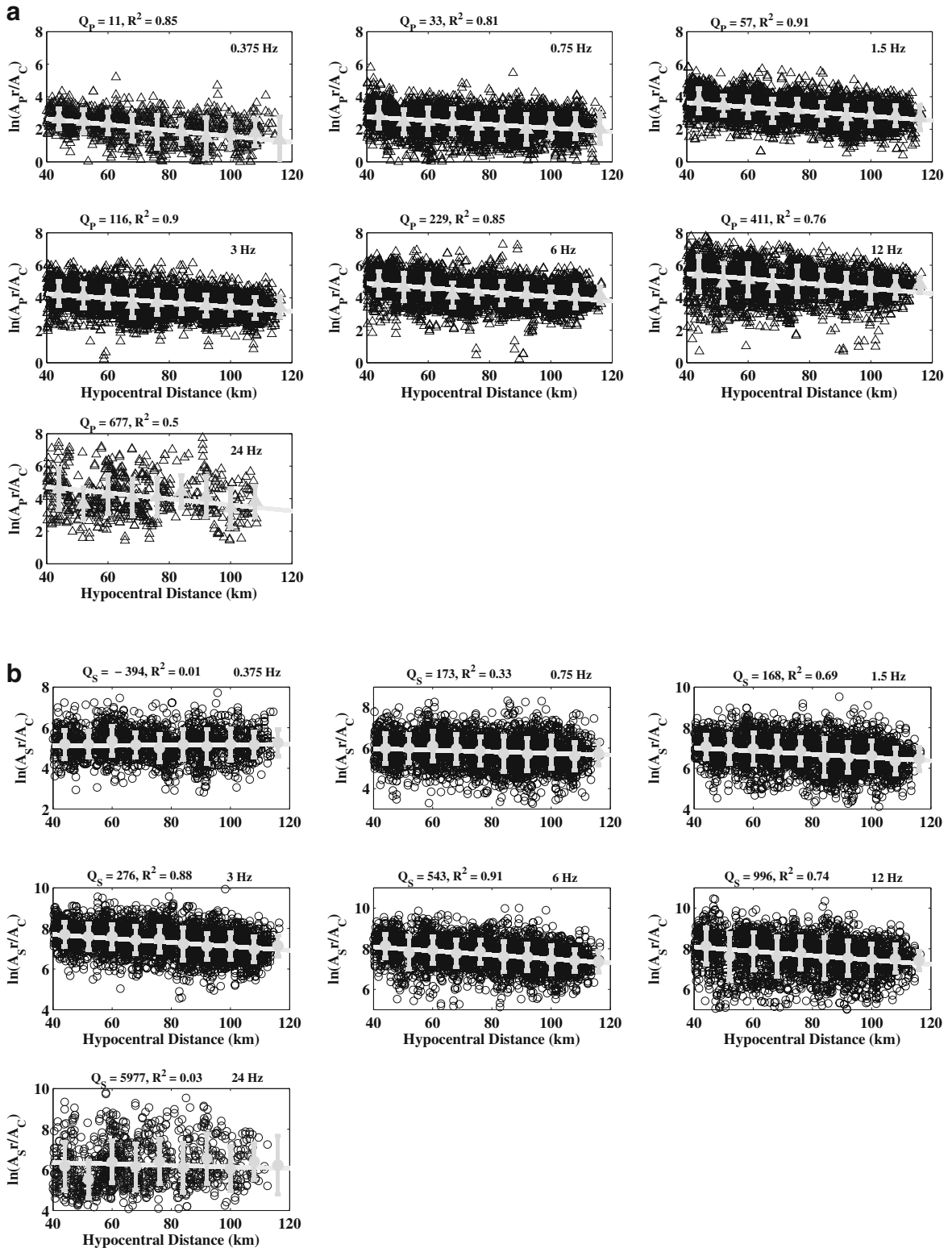
Fig. 4 Plot of the left-hand side of Eqs. (2) and (3) against hypocentral distance for **a** P waves and **b** S waves, respectively. The regression lines are expressed by *solid lines*
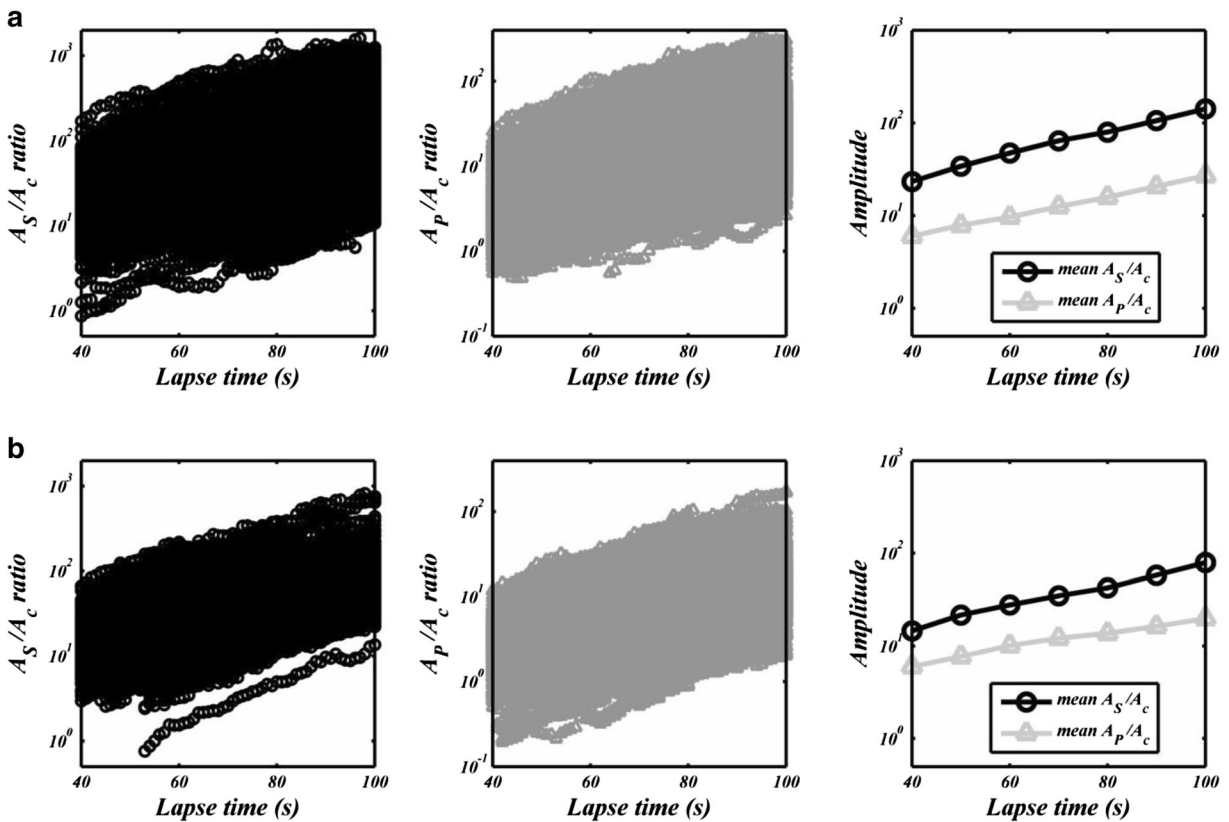
Fig. 5 Normalized amplitude of P (A_P/A_c) and S waves (A_S/A_c) is plotted versus lapse time for **a** Alborz region and **b** North Central Iran at 6 Hz. The mean value of A_P/A_c and A_S/A_c can be observed at the right end of figure. *Triangles* and *circles* are related to P and S waves, respectively

Intrinsic absorption, scattering attenuation, and total attenuation are considered for frequency of 6.3 Hz as 1/220, 1/523, and 1/178, respectively (de Lorenzo et al. 2013). It was observed that the estimated values of Q are lapse time independent based on the synthetic seismogram envelopes (Fig. 8d). We observed the lapse time independency of Q for both observed and synthesized seismograms. This lapse time independency at lapse times 40 to 100 s is related to this fact that the energy of seismic waves is similarly attenuated at the applied distance range (30–130 km).

The frequency-dependent relationships of Q_P and Q_S values in this study have been compared with other results (Fig. 9) in Iran (Motazedian 2006; Zarean et al. 2008; Shoja Taheri and Farrokhi 2009; Mahood et al. 2009; Motaghi and Ghods 2012). The quality factors estimated for Alborz region and North Central Iran are higher compared to other regions of Iran. This shows that direct seismic wave attenuations in these regions are less than those in other parts of Iran. The frequency-dependent relationships of Q_P and Q_S, which have been

estimated for North Central Iran, are comparable with Mahood et al. (2009) for east Central Iran. The similarity is due to this fact that these two regions are related to the same seismotectonic province of Central Iran (Berberian 1976).

The estimated Q_S values are bounded between the results of Motaghi and Ghods (2012) and Motazedian (2006) in Alborz region. We used extended CNM to eliminate the effects of source, site, and instrumental response and individually estimate the attenuation of P and S waves. While, the other researchers used ground motion attenuation relation, which can be used for simultaneous estimation of source, site, GS, and anelastic attenuation. The trade-off between different parameters of ground motion attenuation relation may affect the attenuation estimation. Motaghi and Ghods (2012) overestimate the attenuation properties. This overestimation was partly due to considering higher shear wave velocity of 3.7 km/s, which consequently results in lower Q_S values. It is well known that the Q value increases with increasing distance. While, Motaghi and Ghods (2012)

Fig. 6 The values of Q_P^{-1} (*triangle*) and Q_S^{-1} (*circle*) estimated at different lapse times in Alborz region
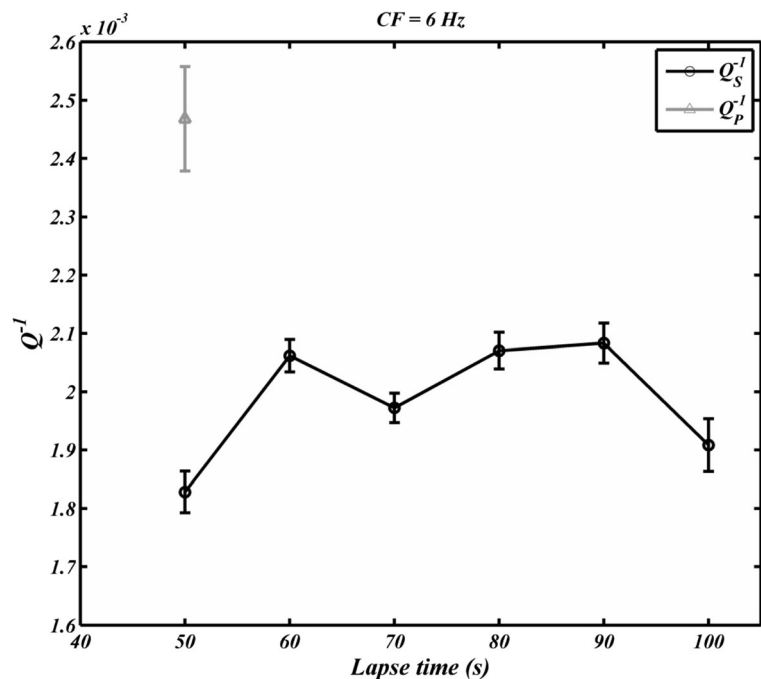
did not consider the effect of different distance ranges in the Q estimation. Motazedian (2006) underestimated the attenuation properties, which seem to be related to inappropriate data selection (Motaghi and Ghods 2012).

We observed that the estimated Q_P and Q_S values of Alborz region are higher than those of North Central Iran (Fig. 9). Station correction of ground motion attenuation relation for the similar area (Motaghi and Ghods 2012) confirms our results. This spatial variation of Q values may be due to the different geological or lithospheric structures. Motaghi and Ghods (2012) reported that the attenuations within the North Central Iran are higher than those of Alborz region and related these differences to geological environmental of each region. They explained that the variation of station correction can be related to the change in the local geology. The North Central Iran is mainly composed of Cenozoic-Quaternary evaporates of

Qom formation (National Iranian Oil Company 1977, 1978). The rocks existed within the Alborz region are mostly composed of older Paleozoic rocks or consolidated Tertiary volcanic rocks of Karaj formation (National Iranian Oil Company 1977, 1978). It has been known that evaporates (salt and gypsum, etc.) have higher attenuation properties compared to the consolidated volcanic rocks. Therefore, the variation between the two regions may be a result of local geology (Motaghi and Ghods 2012). By investigation of coda wave attenuation, Rahimi et al. (2010) concluded that the deeper regions of Central Iran's lithosphere are more attenuative compared to the Alborz region. This result has been approved by surface wave tomography (Rahimi et al. 2014). The results of Rahimi et al. (2014) explained that a shallow asthenosphere existed beneath the Central Iran (66–137-km depth). The existence of shallow asthenosphere beneath Central Iran may result in the high seismic attenuation of this region compared to the Alborz region.

Comparison of the estimated Q_S and Q_c values reported for this region ($Q_c = 105f^{0.93}$: Farrokhi et al. 2015) indicates that the direct waves mostly attenuate due to the effect of intrinsic attenuation (Farrokhi et al. 2016). The anelastic attenuation

Table 2 Frequency-dependent relationships for the studied area

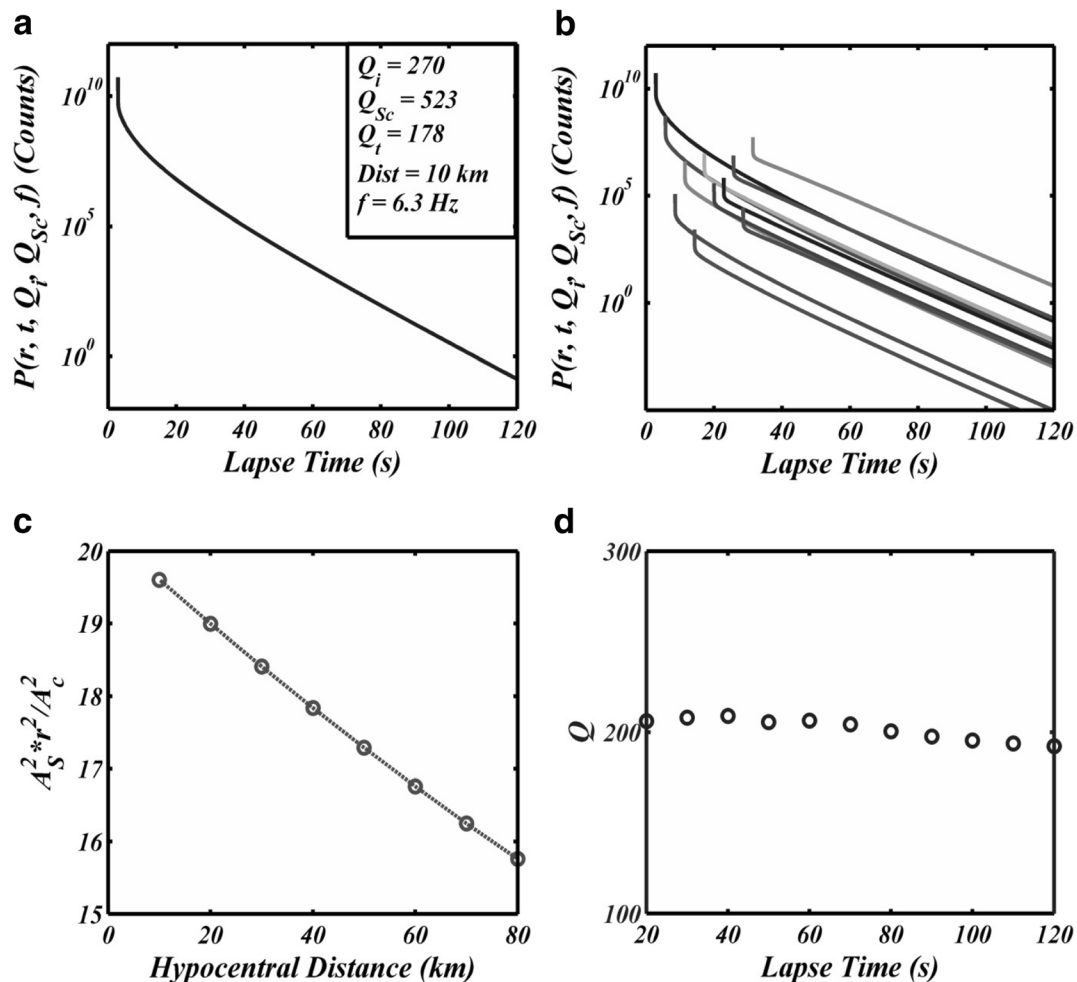| Region	Q_P	Q_S
Alborz region	$62 \pm 7 f^{1.03 \pm 0.07}$	$83 \pm 8 f^{0.99 \pm 0.07}$
North Central Iran	$48 \pm 5 f^{0.95 \pm 0.07}$	$68 \pm 5 f^{0.96 \pm 0.05}$
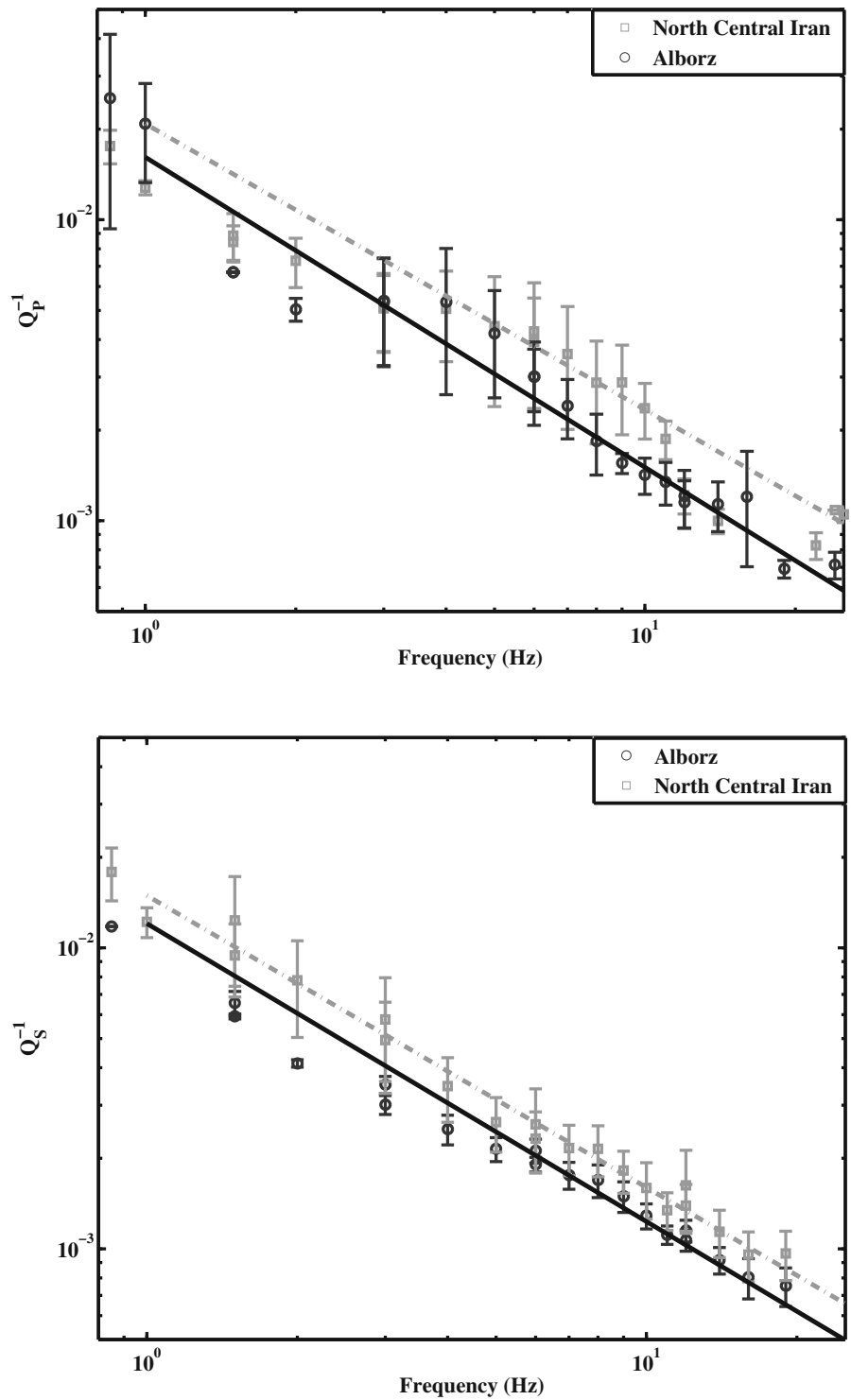
Fig. 8 a Synthetic envelope of intensity calculated using the Paasschens (1997) approximation for a half space at 10 km. b Envelopes of seismograms with hypocentral distances from 10 to 110 km for a half space. c The regression of normalized intensity of S waves by coda waves versus hypocentral distances at lapse time of 50 s. d The estimated Q at lapse times from 30 to 120 s for synthetic seismograms without noise. The following data are considered in the calculation: $Q_i = 270$, $Q_{Sc} = 523$, and $Q_t = 178$

changes due to the existence of cracks, fluid saturation of rocks, thermoelastic effects,… (Jackson and Anderson 1974). The thermoelastic effect results in high dissipation of seismic waves due to partial melting,… (Jackson and Anderson 1974). The existence of Quaternary Damavand volcano is the result of such thermal effects. This young magmatism could be the origin of high attenuation observed. Mostafanejad et al. (2011) reported a low-velocity zone in the eastern part of Damavand volcano and reported that region to the Damavand magma chamber. The low Q values may be partly associated with viscosity and thermal relaxation due to the thermoelastic effects and partly originated from the tectonic forces, existing faults, and fractures within the crust.

The low Q_0 values ($Q_0 < 200$) and high-frequency dependency (n) have been observed for tectonically active regions (Fedotov and Boldyrev 1969; Console and Rovelli 1981; Rebollar et al. 1985; Yoshimoto et al. 1993; Del Pezzo et al. 1995; Yoshimoto et al. 1998; Martynov et al. 1999; Bindi et al. 2006; Sharma et al. 2008). The high Q_0 value ($Q_0 > 600$) and low-frequency dependency (n) have been reported for tectonically stable regions (Kvamme and Havskov 1989; Sarker and Abres 1998; Chung and Sato 2001; Jeon and Herrmann 2004). The estimated values of Q_P and Q_S have been compared with the results of other regions of the world (Fig. 10). The estimated values of Q_P and Q_S are similar to tectonically active regions.
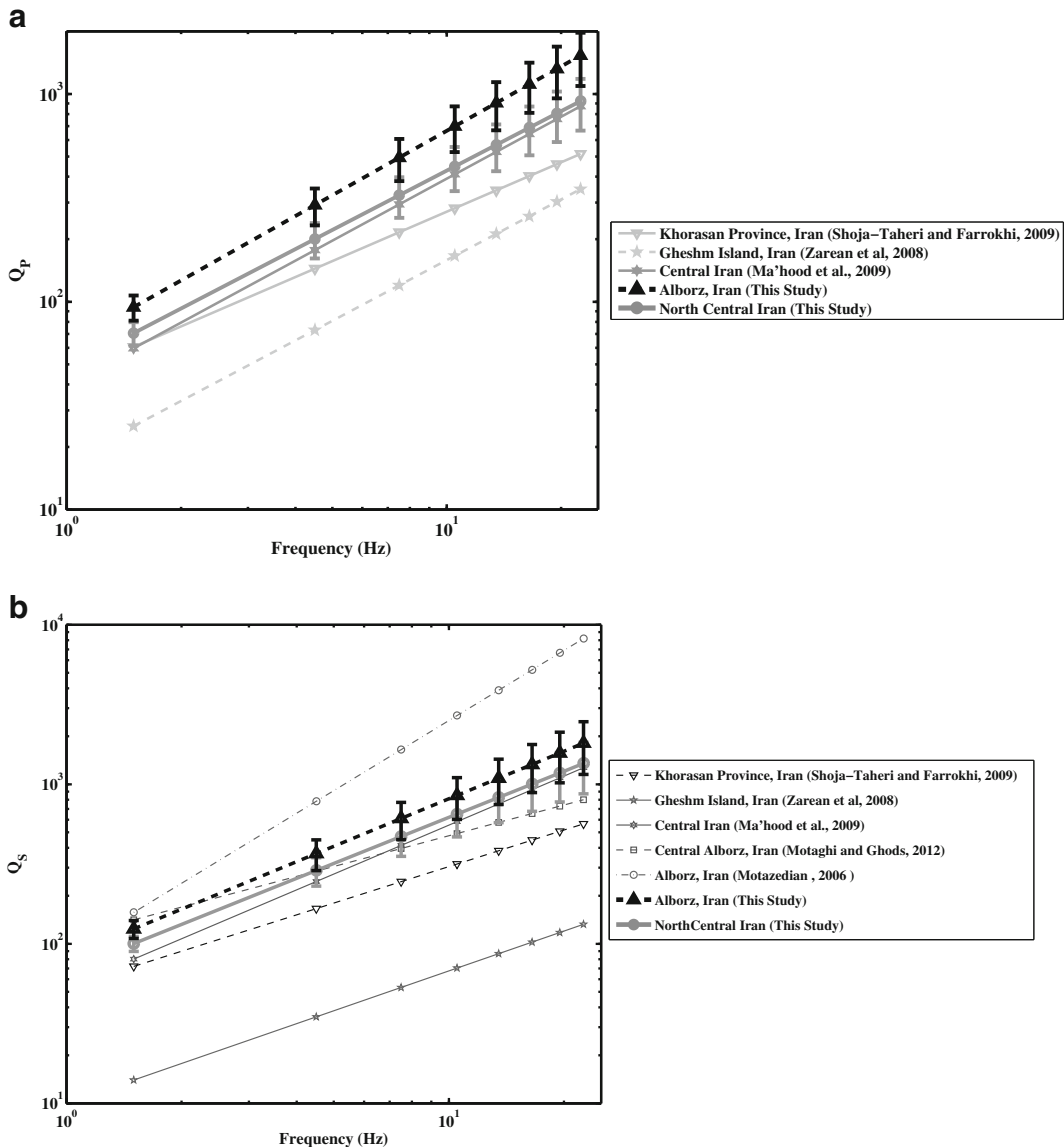
Fig. 9 Comparison of estimated values of quality factor with other regions of Iran for **a** P waves (Q_P) and **b** S waves (Q_S)

7 Conclusions

The quality factors of P and S waves were investigated within the Alborz region and North Central Iran using extended CNM. Based on the analysis of 14,000 waveforms, the following conclusions were emerged:

- The estimated Q values show high-frequency dependence. The frequency dependence of Q_P was

determined in the form of $62 \pm 7 f^{1.03 \pm 0.07}$ and $48 \pm 5 f^{0.95 \pm 0.07}$ in the Alborz region and North Central Iran, respectively. These relationships for Q_S are in the form of $83 \pm 8 f^{0.99 \pm 0.07}$ and $68 \pm 5 f^{0.96 \pm 0.05}$ in Alborz region and North Central Iran, respectively.

- The lapse time dependency of the estimated Q_P and Q_S values was investigated by using 61 normalization coda windows. It has been observed that the
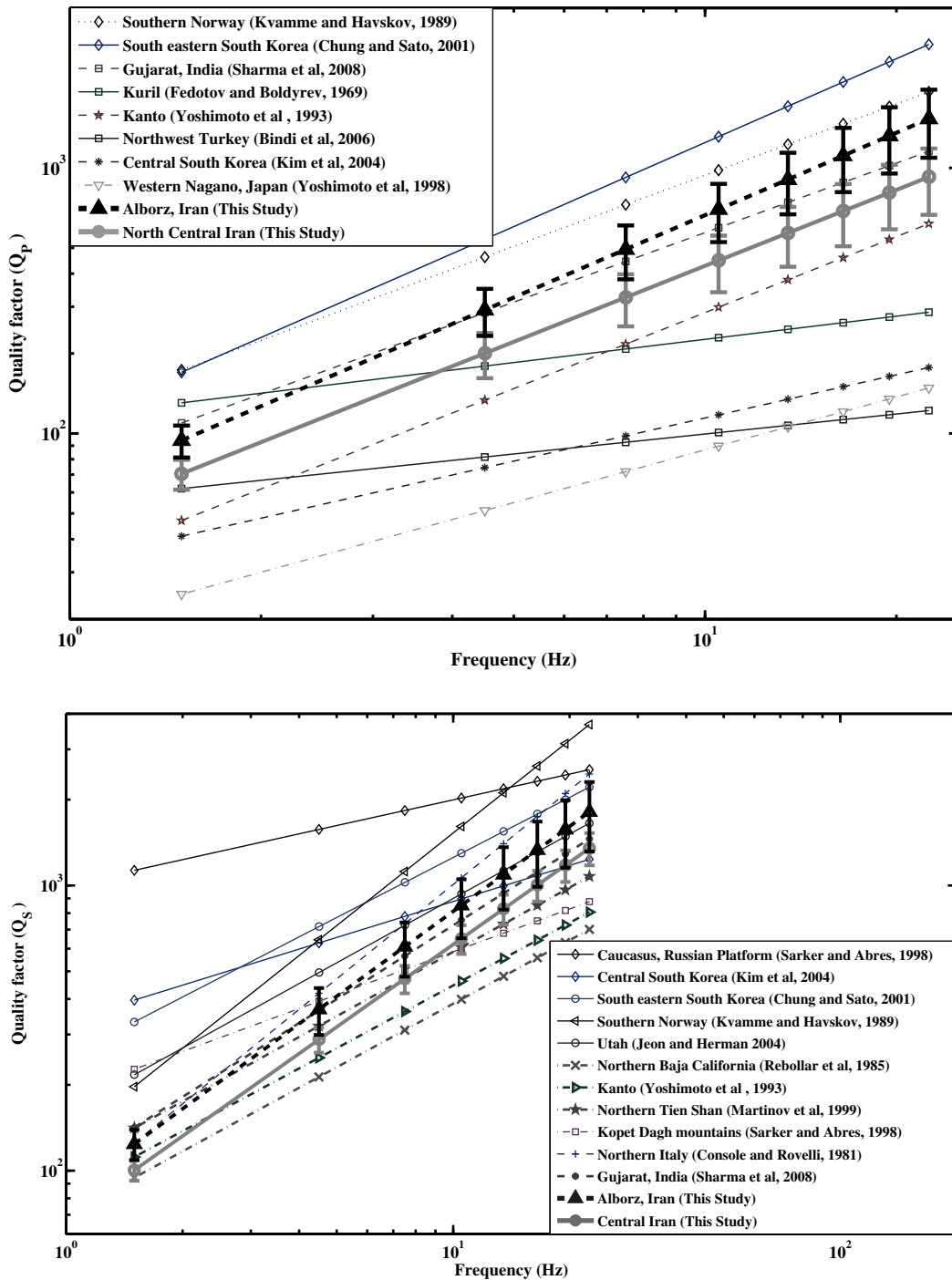
Fig. 10 Comparison of estimated with other regions of world for Q_P (*top*) and Q_S values (*bottom*)

estimated Q_P and Q_S values are not depending on the used lapse time for hypocentral distance range of 30 to 130 km. The similar results were observed by analyzing synthesized waveforms. It was observed

that the estimated Q values are lapse time independent for distance of 30 to 130 km.

• Despite the low Q values estimated for the studied area, it was also observed that the attenuation of

direct waves in this region is less than other parts of Iranian plateau.

• The Q values estimated for P and S waves are similar to the tectonically active regions of the world.

References

Aki K (1969) Analysis of the seismic coda of local earthquakes as scattered waves. J Geophys Res 74:615–631

Aki K (1980) Attenuation of shear-waves in the lithosphere for frequencies from 0.05 to 25 Hz. Phys Earth Planet Inter 21:50–60

Aki K (1992) Scattering conversions P to S versus S to P. Bull Seism Soc Am 82:1969–1972

Aki K, Chouet B (1975) Origin of coda waves: source, attenuation, and scattering effects. J Geophys Res 80:3322–3342

Allen MB, Ghassemi MR, Sharabi M, Qoraishi M (2003) Accommodation of late Cenozoic oblique shortening in the Alborz range, northern Iran. J Struct Geol 25:659–672

Ambraseys NN, Melville CP (1982) A history of Persian earthquakes. Cambridge University Press, London

Ballato P, Uba CE, Landgraf A, Strecker MR, Sudo M, Stockli DF, Friedrich A, Tabatabaei SH (2011) Arabia-Eurasia continental collision: insights from late Tertiary foreland-basin evolution in the Alborz Mountains, northern Iran. Geol Soc Am Bull 123:106–131

Berberian M (1976) Contribution to the seismotectonics of Iran (part II), Geological Survey of Iran, Report No. 39

BHRC (2007) Iranian code of practice for seismic resistant design of buildings (Standard No. 2800—3rd edition), Building and Housing Research Center (BHRC) publication No. S 465, Tehran, Iran

Bianco F, Del Pezzo E, Castellano M, Ibanez J, Di Luccio F (2002) Separation of intrinsic and scattering seismic attenuation in the Southern Apennine zone, Italy. Geophys J Int 150:10–22

Bindi S, Parolai D, Grosser H, Milkereit C, Karakisa S (2006) Crustal attenuation characteristics in northwestern Turkey in the range 1 to 10 Hz. Bull Seis Soc Am 96:200–214

Chung TW, Lee K (2003) A study of high-frequency Q_{Lg}^{-1} in the crust of South Korea. Bull Seis Soc Am 93:1401–1406

Chung TW, Sato H (2001) Attenuation of high-frequency P and S waves in the crust of the southeastern South Korea. Bull Seis Soc Am 91:1867–1874

Console R, Rovelli A (1981) Attenuation parameters for Furiuli region from strong motion accelerogram spectra. Bull Seis Soc Am 71:1981–1991

de Lorenzo S, Del Pezzo E, Bianco F (2013) Qc, Qβ, Qi and Qs attenuation parameters in the Umbria-Marche (Italy) region. Phys Earth Planet Inter 218:19–30

Davidson J, Hassanzadeh J, Berzins R, Stockli DF, Bashukooh B, Turrin B, Pandamouz A (2004) The geology of Damavand volcano, Alborz Mountains, northern Iran. Geol Soc Am Bull 116:16–29

Del Pezzo E, Ibanez J, Morales J, Akinci A, Maresca R (1995) Measurements of intrinsic and scattering seismic attenuation in the crust. Bull Seismol Soc Am 85:1373–1380

Del Pezzo E, Bianco F, De Siena L, Zollo A (2006) Small scale shallow attenuation structure at Mt. Vesuvius, Italy. Phys Earth Planet Inter 157:257–268

Farrokhi M, Hamzehloo H, Rahimi H, Allameh Zadeh M (2015) Estimation of coda wave attenuation in the Central and Eastern Alborz, Iran. Bull Seis Soc Am 105:1756–1767

Farrokhi M, Hamzehloo H, Rahimi H, Allameh Zadeh M (2016) Separation of intrinsic and scattering attenuation in the crust of central and eastern Alborz region, Iran. Phys Earth Planet Inter 253:88–96

Fedotov SA, Boldyrev SA (1969) Frequency dependence of the body-wave absorption in the crust and the upper mantle of the Kuril Island chain. Izv Acad Sci USSR (Engl trans Phys Solid Earth) 9:17–33

Frankel A, McGarr A, Bicknell J, Mori J, Seeber L, Cranswick E (1990) Attenuation of high-frequency shear waves in the crust: measurements from New York State, South Africa, and southern California. J Geophys Res: Solid Earth 95:17441–17457

Guest B, Guest A, Axen G (2007) Late Tertiary tectonic evolution of northern Iran: a case for simple crustal folding. Glob Planet Chang 58:435–453

Hamzehloo H, Rahimi H, Sarkar I, Mahood M, Mirzaei Alavijeh H, Farzanegan E (2010) Modeling the strong ground motion and rupture characteristics of the March 31, 2006, Darb-e-Astane earthquake, Iran, using a hybrid of near-field SH-wave and empirical Green's function method. J Seismol 14:169–195

Hermanns RB, Kijko A (1983) Modelling some empirical vertical component L_g relations. Bull Seis Soc Am 73:157–171

Jackson DD, Anderson DL (1974) Physical mechanism of seismic-waves attenuation. Review of Geophysics and Space and Space Physics 8:1–63

Jackson J, McKenzie D (1984) Active tectonics of the Alpine–Himalayan belt between western Turkey and Pakistan. Geophys J R Astron Soc 77:185–264

Jeon YS, Herrmann RB (2004) High-frequency earthquake ground-motion scaling in Utah and Yellowstone. Bull Seis Soc Am 94:1644–1657

Jin A, Aki K (1988) Spatial and temporal correlation between coda Q and seismicity in China. Bull Seismol Soc Am 78:741–769

Kamalian N, Hamzehloo H, Ghasemi H (2007) S-wave attenuation and spectral decay parameter for the Avaj region, Iran. Iranian Journal of Science & Technology, Transaction A 31:63–71

Kim KD, Chung TW, Kyung JB (2004) Attenuation of high frequency P and S waves in the crust of Choongchung

province, Central South Korea. Bull Seis Soc Am 94: 1070–1078

Knopoff L (1964) Q Review of Geophysics 2:625–660

Kumar N, Parvez IA, Virk H (2005) Estimation of coda wave attenuation for NW Himalayan region using local earthquakes. Phys Earth Planet Inter 151:243–258

Kvamme LB, Havskov J (1989) Q in southern Norway. Bull Seis Soc Am 79:1575–1588

Lay T, Wallace TC (1995) Modern global seismology. Academic Press Inc, San Diego, USA

Lienert BRE, Havskov J (1995) A computer program for locating earthquakes both locally and globally. Seismol Res Lett 66:26–36

Mahood M, Hamzehloo H, Doloei GJ (2009) Attenuation of high frequency P and S waves in the crust of the East-Central Iran. Geophys J Int 179:1669–1678

Martynov VG, Vernon FL, Mellors RJ, Pavlis GL (1999) High frequency attenuation in the crust and upper mantle of the northern Tien Shan. Bull Seis Soc Am 89:215–238

Mostafanejad A, ZH Shomali AA Mottaghi 3-D velocity structure of Damavand volcano, Iran, from local earthquake tomography. J Asian Earth Sci, 2011. 42: 1091-1096.

Motaghi K, Ghods A (2012) Attenuation of ground-motion spectral amplitudes and its variations across the Central Alborz Mountains. Bull Seis Soc Am 102:1417–1428

Motazedian D (2006) Region-specific key seismic parameters for earthquakes in northern Iran. Bull Seis Soc Am 96:1383–1395

Mukhopadhyay S, Tyagi C (2007) Lapse time and frequency-dependent attenuation characteristics of coda waves in the Northwestern Himalayas. J Seismol 11:149–158

Naghavi M, Shomali ZH, Zare M (2012) Lg coda variations in North-Central Iran. International Journal of Geophysics 2012:1–7

National Iranian Oil Company (NIOC) (1977) Geological map of Iran sheet 2: North-Central Iran, scale 1:1, 000,000

National Iranian Oil Company (NIOC) (1978) Geological map of Iran sheet 1: North-West Iran, scale 1:1,000,000

Paasschens J (1997) Solution of the time-dependent Boltzmann equation. Phys Rev E 56:1135–1141

Pulli JJ (1984) Attenuation of coda waves in New England. Bull Seismol Soc Am 74:1149–1166

Radjaee A, Rham D, Mokhtari M, Tatar M, Priestley K, Hatzfeld D (2010) Variation of Moho depth in the central part of the Alborz Mountains, northern Iran. Geophys J Int 181:173–184

Rahimi H, Motaghi K, Mukhopadhyay S, Hamzehloo H (2010) Variation of coda wave attenuation in the Alborz region and Central Iran. Geophys J Int 181:1643–1654

Rahimi H, Hamzehloo H, Vaccari F, Panza GF (2014) Shear-wave velocity tomography of the lithosphere–asthenosphere system beneath the Iranian plateau. Bull Seis Soc Am 104:2782–2798

Rautian T, Khalturin V (1978) The use of the coda for determination of the earthquake source spectrum. Bull Seismol Soc Am 68:923–948

Rebollar CJ, Traslosheros C, Alvarez R (1985) Estimates of seismic wave attenuation in Northern Baja California. Bull Seis Soc Am 75:1371–1382

Ritz JF, Nazari H, Ghassemi A, Salamati R, Shafei A, Solaymani S, Vernant P (2006) Active transtension inside Central Alborz: a new insight into northern Iran–southern Caspian geodynamics. Geology 34:477–480

Sarker G, Abres GA (1998) Comparison of seismic body wave and coda wave measures of Q. Pure Appl Geophys 153:665–683

Sato H (1977) Energy propagation including scattering effects: single isotropic approximation. J Phys Earth 25:27–41

Sato H, Fehler MC (2008) Earth heterogeneity and scattering effects on seismic waves. Springer-Verlag, New York

Sato H, Fehler MC, Maeda T (2012) Seismic wave propagation and scattering in the heterogeneous earth. Springer, New York, USA

Sens-Schönfelder C, Wegler U (2006) Radiative transfer theory for estimation of the seismic moment. Geophys J Int 167:1363–1372

Sharma B, Gupta KA, Devi KD, Kumar D, Teotia SS, Rastogi BK (2008) Attenuation of high frequency seismic waves in Kachchh region, Gujarat, India. Bull Seis Soc Am 98: 2325–2340

Shoja Taheri J, Farrokhi M (2009) Attenuation of high frequency P and S waves in Khorasan Province in Iran. in SSA annual meeting, Monterey, California. Seis Res Lett 80(2):346

Singh S, Herrmann RB (1983) Regionalization of crustal coda Q in the continental United States. J Geophys Res 88:527–538

Sodoudi F, Yuan X, Kind R, Heit B, Sadidkhouy A (2009) Evidence for a missing crustal root and a thin lithosphere beneath the Central Alborz by receiver function studies. Geophys J Int 177:733–742

Stöcklin J (1974) Possible ancient continental margin in Iran. In: Burke C, Drake C (eds) Geology of continental margins. Springer-Verlag, New York

Tsujiura M (1978) Spectral analysis of the coda waves from local earthquakes. Bull Earthq Inst Univ Tokyo 53:1–48

Ugalde A, Carcolé E, Vargas CA (2010) S-wave attenuation characteristics in the Galeras volcanic complex (south western Colombia). Phys Earth Planet Inter 181:73–81

Vernant P, Nilforoushan F, Chery J, Bayer R, Djamour Y, Masson F, Nankali H, Ritz JF, Sedighi M, Tavakoli F (2004) Deciphering oblique shortening of central Alborz in Iran using geodetic data. Earth Planet Sci Lett 223:177–185

Wu RS (1985) Multiple scattering and energy transfer of seismic waves—separation of scattering effect from intrinsic attenuation—I. Theoretical modelling. Geophys J R Astr Soc 82: 57–80

Yoshimoto K, Sato H, Ohtake M (1993) Frequency-dependent attenuation of P and S waves in the Kanto area, Japan, based on the coda-normalization method. Geophys J Int 114:165–174

Yoshimoto K, Sato H, Iio Y, Ito H, Ohminato T, Ohtake M (1998) Frequency-dependent attenuation of high-frequency P and S waves in the upper crust in western Nagano, Japan. Pure Appl Geophys 153:489–502

Zarean A, Farrokhi M, Chaychizadeh S (2008) Attenuation of high frequency P and S waves on Qeshm Island, Iran. in 14th World Conference on Earthquake Engineering, Beijing, China

Zeng Y (1991) Compact solution for multiple scattered wave energy in time domain. Bull Seis Soc Am 81:1022–1029